ChemistryOPEN Full Papers

ChemPubSoc Europe

Open Access

DOI: 10.1002/open.201402076

Design, Synthesis, and Biological Evaluation of Tetra-Substituted Thiophenes as Inhibitors of p38α MAPK

Natalie B. Vinh,[a] Shane M. Devine,[a] Lenka Munoz,[b] Renae M. Ryan,[b] Bing H. Wang,[c] Henry Krum,[c] David K. Chalmers,[a] Jamie S. Simpson,[a] and Peter J. Scammells*[a]

p38α mitogen-activated protein kinase (MAPK) plays a role in several cellular processes and consequently has been a therapeutic target in inflammatory diseases, cancer, and cardiovascular disease. A number of known p38α MAPK inhibitors contain vicinal 4-fluorophenyl/4-pyridyl rings connected to either a 5- or 6-membered heterocycle. In this study, a small library of substituted thiophene-based compounds bearing the vicinal 4-fluorophenyl/4-pyridyl rings was designed using computational docking as a visualisation tool. Compounds were synthesised and evaluated in a fluorescence polarisation binding assay. The synthesised analogues had a higher binding affinity to the active phosphorylated form of p38α MAPK than the inactive nonphosphorylated form of the protein. 4-(2-(4-fluorophenyl)thiophen-3-yl)pyridine had a K_i value of 0.6 μM to active p38α MAPK highlighting that substitution of the core ring to a thiophene retains affinity to the enzyme and can be utilised in p38α MAPK inhibitors. This compound was further elaborated using a substituted phenyl ring in order to probe the second hydrophobic pocket. Many of these analogues exhibited low micromolar affinity to active p38α MAPK. The suppression of neonatal rat fibroblast collagen synthesis was also observed suggesting that further development of these compounds may lead to potential therapeutics having cardioprotective properties.

Introduction

p38α Mitogen-activated protein kinase (MAPK) is a serine threonine protein kinase that regulates multiple cellular processes.[1] Although this ubiquitous kinase has primarily been targeted for its role in inflammatory diseases,[2] p38α MAPK activity has also been linked to cardiovascular disease as it coordinates the myocardial stress response to various stimuli including inflammatory, ischemic, mechanical, oxidative, neurohumoral, and pharmacological stressors.[3] Pharmacological inhibition of p38α MAPK has been shown to improve cardiac function and reduce cardiac remodelling post myocardial infarction or cardiac injury.[4]

The structure of p38α MAPK is typical of most protein kinases consisting of *N*- and *C*-terminal domains that are connected by a hinge region (His107–Asp112).[5] The ATP binding site is formed by the interface between the two domains with the hinge region as its border. This binding site is made up of an adenine binding region, sugar pocket, phosphate binding region, and two hydrophobic pockets.[6] One hydrophobic pocket contains a 'gatekeeper' residue. In p38α MAPK this residue is a threonine (Thr106), which is smaller than the corresponding methionine or glutamine seen in p38γ, p38δ, extracellular-signal-regulated kinases (ERKs), and c-Jun N-terminal kinases (JNKs).[2b,7] An example of a p38α MAPK inhibitor that utilises this pocket is SB203580 (Figure 1), which has an IC_{50} value of 74 nM.[8] In this compound the 4-fluorophenyl substituent fits optimally in the hydrophobic pocket. Along with this key interaction, SB203580 contains a 4-pyridyl ring that occupies the adenine binding region and forms a key hydrogen bond with the Met109 amide in the hinge region. The vicinal 4-fluorophenyl and 4-pyridyl rings present in SB203580 are also found in many other p38α MAPK inhibitors and are often connected by a 5- or 6-membered heterocycle. Other interactions of SB203580 include a hydrogen bond between the imidazole core and the Lys53 side chain and π-stacking interactions between the 4-methylsulfinylphenyl moiety and the Tyr35 side chain in the phosphate binding region.[7a]

Although SB203580 inhibits the p38α and p38β MAPK isoforms and not p38γ or p38δ MAPK isoforms, it was later shown to interfere with other protein kinases.[9] Other pyridinyl imidazoles have displayed higher potency and selectivity including RWJ67657 (Figure 2), which has an IC_{50} of 30 nM.[10] An

[a] N. B. Vinh, Dr. S. M. Devine, Dr. D. K. Chalmers, Dr. J. S. Simpson, Prof. P. J. Scammells
Medicinal Chemistry, Monash Institute of Pharmaceutical Sciences
Monash University, 381 Royal Parade, Parkville, VIC 3052 (Australia)
E-mail: Peter.Scammells@monash.edu

[b] Dr. L. Munoz, Dr. R. M. Ryan
Discipline of Pharmacology, School of Medical Sciences and Bosch Institute
The University of Sydney, Sydney, NSW 2006 (Australia)

[c] Dr. B. H. Wang, Prof. H. Krum
Centre of Cardiovascular Research and Education in Therapeutics
Department of Epidemiology and Preventative Medicine
Monash University, 99 Commercial Road, Melbourne, VIC 3004 (Australia)

Supporting information for this article is available on the WWW under http://dx.doi.org/10.1002/open.201402076.

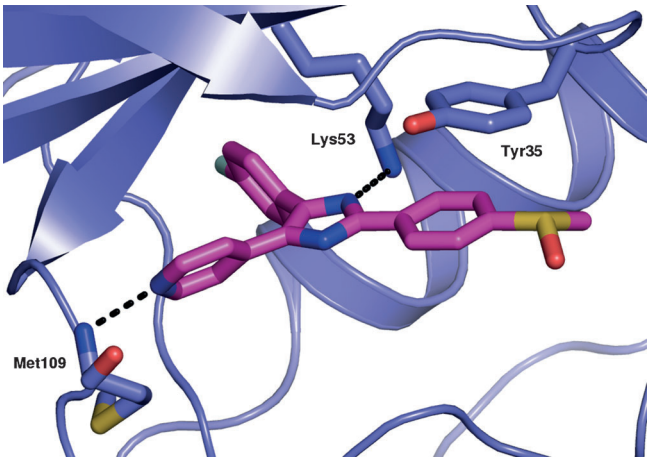

Figure 1. Crystal structure 1A9U[7a] shows SB203580 in the ATP pocket of p38α MAPK.

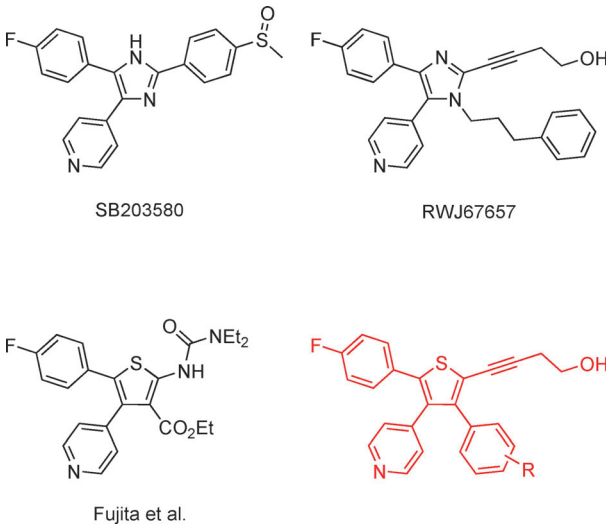

Figure 2. Structures of the p38α MAPK inhibitors: SB203580[8] and RWJ67657,[14] and the thiophene-based TNF-α suppressor synthesised by Fujita et al.[13] The general structure of the designed ligands is shown in red.

investigation into the specificity of RWJ67657 showed no inhibition of recombinant p38γ or p38δ MAPK isoforms or a number of other protein kinases (ERK2, protein kinase A, p56^{lck}, and c-*src* tyrosine kinases).[11] This compound contains a phenylpropyl group that is thought to bind in the second hydrophobic pocket. Goldstein et al. described structural features of the protein that may be targeted for additional selectivity.[12] As well as the hydrophobic "gatekeeper" pocket, optimising inhibitor binding to the second hydrophobic pocket may contribute to selectivity.[12]

Compounds were designed to target the ATP binding pocket. The diaryl-heterocycle p38α MAPK inhibitor class was investigated in which compounds contained a thiophene core. Fujita et al. synthesised substituted thiophenes and bicyclic compounds possessing the key vicinal 4-fluorophenyl/4-pyridyl rings seen in many p38α MAPK inhibitors.[13] Their substituted thiophene ester shown in Figure 2, was found to suppress TNF-α production with an IC_{50} value of 1.7 μM.[13] By combining characteristics of this TNF-α suppressor with features of a known p38α MAPK inhibitor (RWJ67657,[14] Figure 2), we aimed to synthesise thiophene-based p38α MAPK inhibitors. We also sought to determine whether substitution of the core 5-membered heterocycle with a thiophene could retain p38α MAPK activity. In addition, the second hydrophobic pocket was probed for further interactions using an extra aryl ring.

Computational modelling was used to dock in designed ligands and enable visualisation of their likely binding mode in the p38α MAPK protein. A series of tetra-substituted thiophenes were synthesised and evaluated in a fluorescence polarisation binding assay. Their effect on cardiac fibroblast collagen synthesis was also determined.

Results and Discussion

Molecular Modelling

Although there are more than 200 X-ray crystal structures of p38α MAPK available, the structures exhibit a high degree of ligand-induced conformational changes. As such it was imperative to identify the binding conformation of the protein for the diaryl-heterocycle inhibitor class and to determine which crystal structure is most suitable for docking ligands into the protein. In a previous publication we identified a crystal structure model of p38α MAPK using virtual screening and ensemble docking for the diaryl-heterocycle p38α MAPK inhibitor class bearing 4-fluorophenyl and 4-pyridyl rings.[15] The crystal structure model identified was an ensemble of the 1BL7 and 2EWA crystal structures, which was therefore used for our docking studies.

In this work 53 compounds were designed and docked into the 1BL7 and 2EWA structures, scoring them using our ensemble method. The designed ligands suggested for p38α MAPK inhibition are described in the supporting information. These ligands contained the 4-fluorophenyl/4-pyridyl rings seen in many p38α MAPK inhibitors. In addition a 2-butynyl alcohol substituent, similar to RWJ67657,[14] was used to extend into the polar outer rim of the binding site. A fourth aromatic ring was substituted with hydrogen bond donor or acceptor groups to probe for extra interactions with the protein. Figure 2 illustrates the type of ligands designed and docked into the protein.

Docking was carried out using the Glide v5.6 (Schrödinger) extra precision (XP) method. For the ensemble analysis, the glide scores of the top ranked pose of each ligand in the 1BL7 and 2EWA structures were retained and averaged. The compounds were then re-ranked based on the calculated ensemble scores (see Supporting Information). A visual inspection of the docked compounds within the binding site enabled selection of compounds for synthesis. For example, the top ranked structure was analogue **37** (Figure 3), which contained a *meta*-(2-hydroxyethyl)carbamoyl moiety. Figure 3 shows the docked pose for analogue **37** in the 2EWA crystal structure in which an extra hydrogen bonding interaction is made with the Gly110 backbone amide. Also shown in Figure 3 is the docked pose of

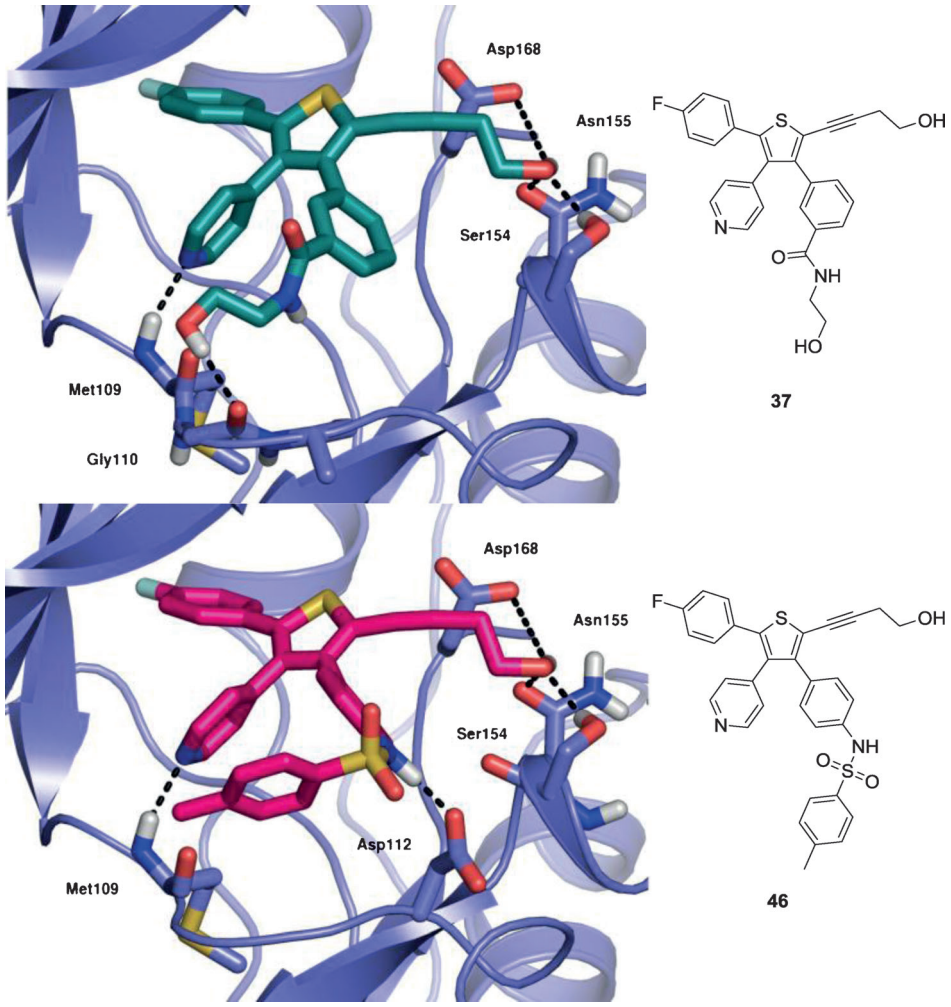

Figure 3. Docked poses of analogue **37** containing a 3-(2-hydroxyethyl)carbamoyl group and analogue **46** containing a *p*-toluenesulfonamide in the 2EWA crystal structure.

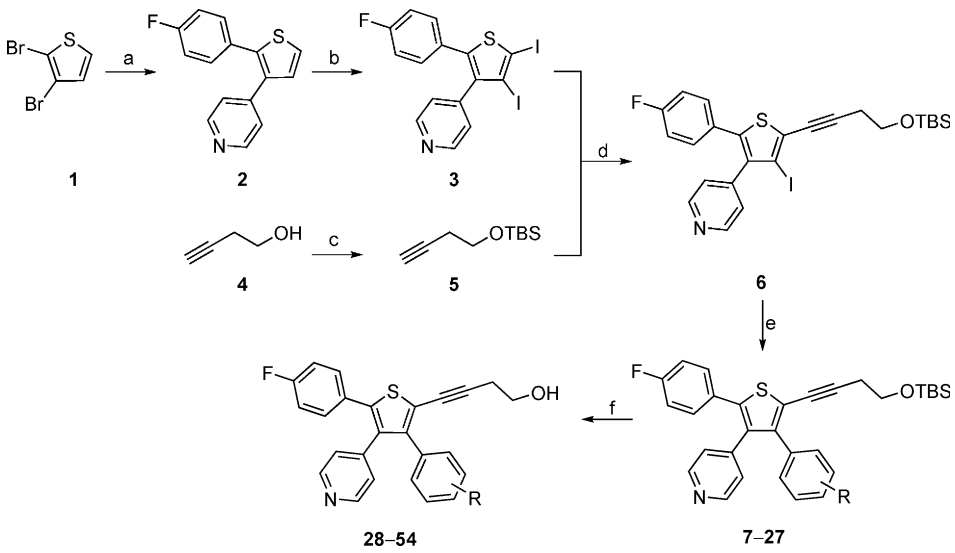

Scheme 1. Synthesis of the tetra-substituted thiophene series. *Reagents and conditions*: a) 1) 4-fluorophenylboronic acid, $PdCl_2(PPh_3)_2$, Na_2CO_3, DMF, H_2O, 70 °C, 3 h; 2) pyridine-4-boronic acid, $PdCl_2(PPh_3)_2$, 120 °C, 16 h, 71%; b) 1) $Hg(OAc)_2$, AcOH, 70 °C, 16 h; 2) KI, I_2, H_2O, THF, 25 °C, 16 h, 81%; c) TBSCl, imidazole, CH_2Cl_2, 25 °C, 16 h, quant.; d) $PdCl_2(PPh_3)_2$, CuI, PPh_3, Et_3N, THF, 70 °C, 2 h, 82%; e) aryl boronic acid, $PdCl_2(PPh_3)_2$, Na_2CO_3 (1 M), THF, μW, 100 °C, 1.5 h, 21–100%; f) NH_4F, MeOH, reflux, 16 h, 58–99%.

analogue **46** bearing a *para*-toluenesulfonamide group. Overall, this compound ranked eighth and it was proposed that an extra hydrogen bond between the amide proton and the Asp112 side chain would be made while the extra toluene group fills the second hydrophobic pocket.

Synthesis

The target thiophenes were synthesised using a series of palladium-catalysed cross coupling reactions, outlined in Scheme 1. Starting with 2,3-dibromothiophene, a one-pot double Suzuki reaction was used to first couple 4-fluorophenylboronic acid, followed by pyridine-4-boronic acid. Coupling at the 3-position proceeded more slowly and required heating at a higher temperature, yielding compound **2** in 71% over the two steps. The thiophene was then halogenated for subsequent palladium-catalysed cross coupling reactions. An organomercury intermediate was used to increase the reactivity of the system to halogenation. Thiophene **2** was reacted with mercuric acetate in acetic acid at 70 °C for 16 h. Once the mercuric acetate intermediate was isolated the compound was reacted with an aqueous solution of potassium triiodide affording 81% of the diiodinated product **3**. Next, a Sonogashira or Negishi coupling reaction was conducted to introduce the alkyne functionality. The Sonogashira reaction was carried out by heating thiophene **3**, *tert*-butyldimethylsilane (TBS)-protected butynyl alcohol **5**, bis(triphenylphosphine)palladium(II) dichloride, copper iodide, triphenylphosphine, and triethylamine in tetrahydrofuran (THF) to give intermediate **6** in 82% yield. Alternatively, the Negishi coupling reaction afforded the same product in 94% yield using thio-

phene **3**, TBS-protected butynyl alcohol **5**, zinc chloride, *n*-butyllithium, and tetrakis(triphenylphosphine)-palladium(0). While the yield for the Negishi coupling reaction was higher, the reaction was more sensitive to moisture. For ease of synthesis the Sonogashira coupling reaction was preferred. With the key intermediate **6** in hand, the Suzuki reaction was used to attach an aromatic ring which would interact with the second hydrophobic pocket. The Suzuki coupling reactions were conducted using bis(triphenylphosphine)palladium(II) dichloride and an excess of the boronic acid under microwave irradiation. Deprotection of the TBS group using ammonium fluoride in methanol at reflux gave the final products (**28**–**54**).

Different substituents on the aryl ring could be incorporated either after the Suzuki reaction or after the TBS deprotection step. We investigated different hydrogen bond donor and acceptor groups in the *ortho*-, *meta*-, and *para*-positions of the aryl ring. As a result of our initial docking studies, a series of carboxy- and amino-phenyl analogues were selected for synthesis. The carboxyphenyl analogues were synthesised from the Suzuki coupling of methylcarboxyphenylboronic acid. Subsequent hydrolysis under basic conditions followed by amide coupling, using (benzotriazol-1-yloxy)tris(dimethylamino)phosphonium hexafluorophosphate (BOP) in the presence of *N*,*N*-diisopropylethylamine (DIPEA), was conducted to form the amide analogues (Scheme 2). The *ortho*-substituted aryl analogues proved difficult to synthesise due to steric hindrance, which resulted in little to no coupling. Analogue **28** was synthesised from the coupling of compound **55** and 2-methoxycarbonylphenyl boronic acid, albeit in poor yield.

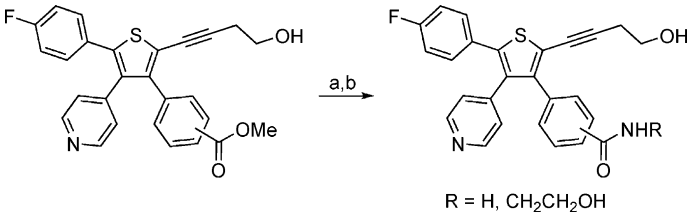

Scheme 2. Synthesis of carboxyphenyl analogues. *Reagents and conditions*: a) NaOH, EtOH, H_2O, 50 °C, 2 h, **31**: 80%, **32**: 92%; b) $(NH_4)_2CO_3$, DMF, BOP, DIPEA, 25 °C, 16 h, **35**: 55%; ethanolamine, BOP, DIPEA, CH_3CN, 25 °C, 16 h, **37**: 57%, **38**: 45%.

The target compounds for the aminophenyl series were synthesised via acylation or sulfonylation of the aniline analogues using acid chloride, anhydride, and sulfonyl chlorides (Scheme 3). None of the desired cross-coupled product was obtained from the Suzuki reaction of compound **6** and 2-aminophenylboronic acid, therefore the *ortho*-substituted analogues were not synthesised.

In addition to the carboxy- and amino-phenyl analogues, a number of diverse boronic acids were used to investigate small ring substituents; these boronic acids were coupled to compound **6** affording analogues **47**–**54** after the removal of the TBS group.

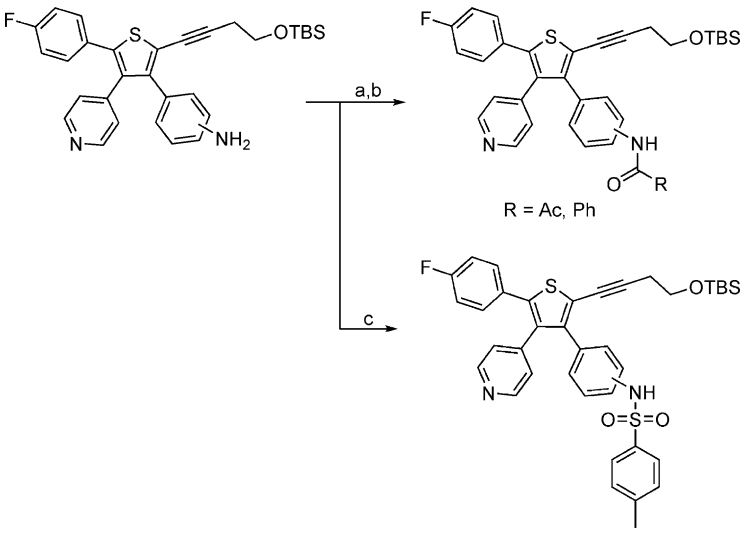

Scheme 3. Synthesis of aminophenyl analogues. *Reagents and conditions*: a) Ac_2O, pyridine, 25 °C, 3 h, **15**: 82%; b) BzCl, Et_3N, EtOAc, 0→25 °C, 4 h, **17**: 88%, **18**: 90%; c) *p*-TsCl, pyridine, CH_2Cl_2, 25 °C, 20 h, **19**: 92%.

Biological Evaluation

Binding affinity to p38α MAPK

The synthesised analogues were evaluated using a fluorescence polarisation (FP) binding assay developed by Munoz et al.[16] using both nonphosphorylated and phosphorylated p38α enzymes. The fluoroprobe used was an analogue of the prototypical p38α inhibitor SB203580 attached to fluorescein. The K_d value for the fluorescently labelled ligand was determined by titrating against increasing concentrations of both the inactive and active forms of p38α MAPK. The fluoroprobe was found to have a K_d value of 13 nM to the inactive protein and 36 nM to the active form of the protein. The binding affinities of compounds **2**, **3** and **28**–**55** are summarised in Table 1.

Most of the synthesised compounds showed little or no binding to the nonphosphorylated protein, however a significant improvement was observed in binding to the phosphorylated enzyme. ATP itself has a low affinity for the inactive p38α enzyme relative to the active form. Since the synthesised analogues are designed to in part mimic some of the interactions ATP makes, namely the hydrogen bond to the Met109 backbone, the analogues are expected to behave similarly. One crystal structure containing the dually phosphorylated p38α MAPK protein exists in the protein databank. Figure 4 illustrates the differences between the apo nonphosphorylated (PDB ID:1P38)[5b] and phosphorylated (PDB ID: 3PY3)[17] p38α MAPK crystal structures. Figure 4 shows that the phosphorylated p38α MAPK structure has a more exposed binding site indicating that the conformational changes in the protein structure that occur as a result of phosphorylation cause the protein to open up in order to accommodate ATP. Therefore, the

Table 1. Binding affinities to inactive and active p38α MAPK.

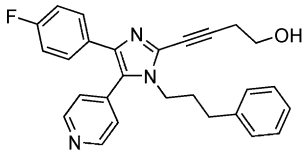

RWJ67657

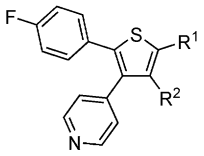

2 R^1 = H
3 R^1 = I
28–55 R^1 = C≡C$(CH_2)_2$OH

Compd	R^2	K_i [μM] inactive p38α[a]	K_i [μM] active p38α[b]
RWJ67657		0.2 ± 0.04	0.01 ± 0.006
2	H	4.4 ± 0.2	0.6 ± 0.1
3	I	> 10	> 10
28	2-(CO_2Me)Ph	> 10	8.7
29	3-(CO_2Me)Ph	> 10	3.0
30	4-(CO_2Me)Ph	> 10	> 10
31	3-(CO_2H)Ph	> 10	7.1
32	4-(CO_2H)Ph	> 10	> 10
33	3-(CH_2OH)Ph	> 10	1.3 ± 0.2
34	4-(CH_2OH)Ph	> 10	3.5
35	3-($CONH_2$)Ph	> 10	2.2 ± 0.3
36	4-($CONH_2$)Ph	> 10	2 ± 1
37	3-(CONH$(CH_2)_2$OH)Ph	1.9 ± 0.2	2 ± 1
38	4-(CONH$(CH_2)_2$OH)Ph	> 10	1.7 ± 0.2
39	3-(NH_2)	> 10	3.2
40	4-(NH_2)	> 10	> 10
41	3-(NHAc)Ph	2.6 ± 0.6	2.0 ± 0.1
42	4-(NHAc)Ph	> 10	> 10
43	3-(NHBz)Ph	> 10	> 10
44	4-(NHBz)Ph	> 10	> 10
45	3-($NHSO_2$*p*toluene)Ph	> 10	> 10
46	4-($NHSO_2$*p*toluene)Ph	> 10	> 10
47	3-(CN)Ph	> 10	1.8 ± 0.4
48	3-(Me)Ph	> 10	> 10
49	4-(NMe_2)Ph	> 10	> 10
50	4-F-Ph	> 10	0.9 ± 0.4
51	4-Cl-Ph	> 10	> 10
52	4-(CF_3)Ph	> 10	> 10
53	4-(Ac)Ph	> 10	2.2 ± 0.3
54	4-OH-Ph	> 10	3.4
55	I	> 10	> 10

Experiments were performed in duplicate with $n = 2$–3 for compounds with K_i values: [a] < 10 μM to inactive p38α and [b] < 3 μM to active p38α. All other compounds were screened in duplicate with $n = 1$.

synthesised analogues may have better access to the ATP pocket once the protein becomes activated, which is reflected in the observed binding affinities.

A comparison of the K_i data to the phosphorylated p38α enzyme shows that analogues containing the methyl ester **29** and acid **31** in the *meta*-position are weak binders with K_i values of 3.0 and 7.1 μM, respectively. Binding was completely lost when these substituents were placed in the *para*-position. Substitution at either the *meta*- or *para*-positions with an amide (**35** and **36**) or 2-(hydroxyethyl)carbamoyl (**37** and **38**) group had similar binding affinities with K_i values between 1.7–2.2 μM. Analogues containing an amino or acetamido group in the *meta* position (**39** and **41**) showed moderate binding. The corresponding *para*-substituted analogues however showed no binding to the protein. Larger substituents

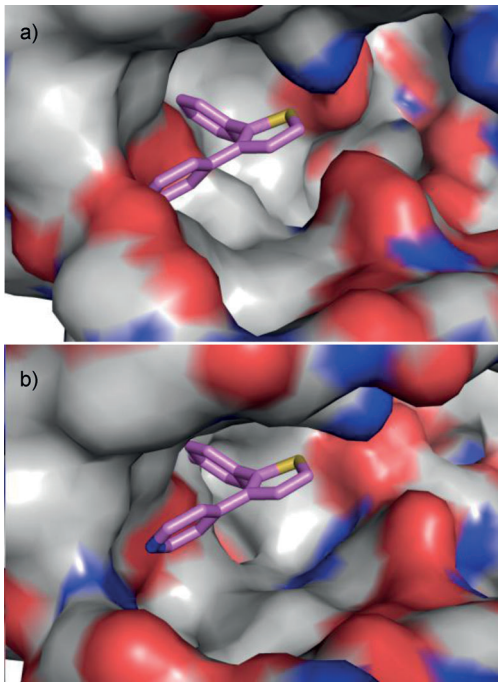

Figure 4. Docked pose of compound **2** in 2EWA overlaid onto: a) nonphosphorylated (inactive) p38α MAPK (PDB: 1P38); b) phosphorylated (active) p38α MAPK (PDB: 3PY3).

such as the benzoylamide or *para*-toluenesulfonamide group were attached to probe space. However these analogues did not bind to the protein. In most cases, substituents that were attached to the *para* position on the aromatic ring were generally poorer binders in comparison to the *meta*-substituted counterparts. Other analogues that demonstrated binding include **47**, **50**, and **53**, which bear a *meta*-cyano, *para*-fluoro, and *para*-acetyl substituents, with K_i values of 1.8, 0.9, and 2.2 μM, respectively. Synthesised intermediates were also evaluated in the binding assay. Interestingly, compound **2** was the best binder, which contained only the 4-fluorophenyl and 4-pyridyl rings attached to the thiophene. This compound had a K_i value of 0.6 μM demonstrating that the conversion to the thiophene core retains affinity to the p38α protein.

Although several analogues displayed moderate affinity to phosphorylated p38α MAPK, the tetra-substituted thiophenes were weaker binders compared to the pyridinyl imidazole RWJ67657 indicating that the proposed substituted phenyl moiety is not optimal in the pocket and further work is required to improve affinity.

Cellular assays

In addition to the binding assay, the effects of the synthesised compounds on cardiac fibroblast collagen synthesis were investigated. Analogues with a K_i value of less than 2.2 μM to active p38α MAPK were evaluated for the inhibition of rat neonatal cardiac fibroblast (NCF) collagen synthesis.[18] p38 MAPK is known to become activated in cardiac cells by a range of stimuli including angiotensin II (AngII).[4a, 19] NCF collagen syn-

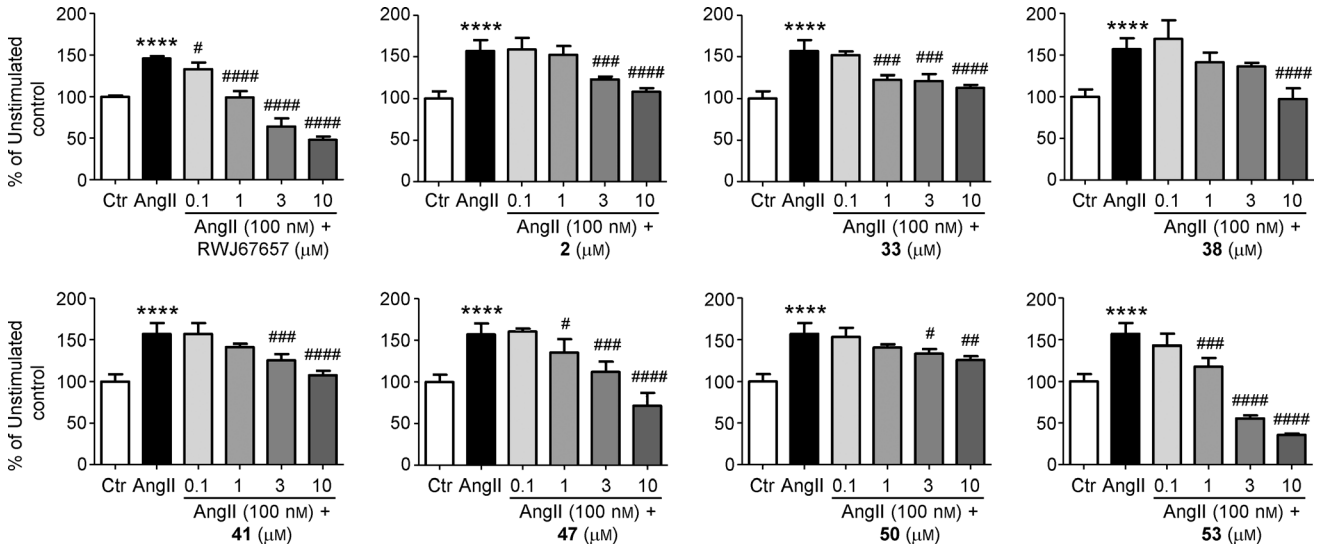

Figure 5. The effects of analogues on neonatal cardiac fibroblast (NCF) collagen synthesis determined by ^{3}H-proline incorporation. NCFs were pre-treated for 2 h with the synthesised analogues at 0.1, 1, 3 and 10 μM, then stimulated by AngII. Data are the mean ± standard error (SEM) with each independent experiment done in triplicate. One-way ANOVA was performed in Graphpad Prism. **** $p < 0.0001$ vs. unstimulated control, # $p < 0.05$, ## $p < 0.01$, ### $p < 0.001$ and #### $p < 0.0001$ vs. stimulated control (AngII).

thesis determined by ^{3}H-proline incorporation, is upregulated in response to AngII stimulation (Figure 5). The cardiac fibroblasts were pre-treated with the synthesised analogues at 0.1, 1, 3, and 10 μM concentrations followed by stimulation with AngII (Figure 5). All of the tested analogues suppressed AngII-stimulated collagen synthesis at 3 and 10 μM concentrations. Few compounds however, inhibited collagen synthesis at 1 μM concentration consistent with the weak binding of the analogues observed in the fluorescence polarisation assay. Compound **53** shows stronger inhibition of collagen synthesis but this may be attributed to other interactions within the cell.

Conclusions

A number of substituted thiophenes were synthesised and shown to bind with higher affinity to the phosphorylated active form of p38α MAPK relative to the nonphosphorylated inactive form. This work shows successful modification of the core to a thiophene with compound **2** having a K_i value of 0.6 μM to the active enzyme. The tetra-substituted thiophene series showed modest inhibition of p38α MAPK with binding affinities in the low micromolar range. These compounds also demonstrate cellular activity; however, further work is required to optimise interactions within the binding pocket and generate more potent compounds. The fact that compound **2**, bearing only the 4-fluorophenyl and 4-pyridyl substituents, displayed the highest affinity suggests that the additional alkyne and aryl substituents are not necessary for binding. Therefore, further alterations to these substituents must be investigated in order to determine whether any stronger or more favourable interactions can be achieved. Optimisation of these substituted thiophenes may lead to p38α MAPK inhibitors that can be used in the treatment of cardiac disease.

Experimental Section

Molecular Modelling–Ensemble Docking

In our previous work we identified the 1BL7–2EWA ensemble as a good model for docking p38α MAPK inhibitors containing the 4-fluorophenyl and 4-pyridyl ring substituents.[15] Therefore, this model was used to dock designed ligands.

The designed ligands suggested for p38α MAPK inhibition were built in ChemBioDraw Ultra 12.0 (CambridgeSoft) and prepared using LigPrep v2.4 (Schrödinger) to convert the two-dimensional structures to their respective three-dimensional structures.

The 1BL7[7a] and 2EWA[20] crystal structures were downloaded from the Protein Data Bank (PDB)[21] and prepared using the Protein Preparation Wizard in Maestro v9.2 (Schrödinger) for the addition of hydrogens and assignment of bond orders and partial charges. Prime v2.2 (Schrödinger) added side chains to residues with missing atoms. Each protein was refined using exhaustive sampling and minimisations were conducted only on the newly added hydrogens.

Docking into both the 1BL7 and 2EWA crystal structures was conducted using the Glide v5.6 (Schrödinger) extra precision (XP) method. For the ensemble analysis, the glidescores of best conformation of each ligand were taken from each crystal structure and averaged. The compounds were re-ranked based on the ensemble score (see Supporting Information).

Chemistry

General remarks: All chemical reagents were acquired from Sigma–Aldrich, Fluka, Merck, Boron Molecular, and Matrix Scientific and were used without further purification. Flash chromatography was carried out using Scharlau silica gel 60, 0.06–0.20 mm (70–230 mesh ASTM). Melting points were determined using a Mettler Toledo MP50 melting point apparatus. NMR spectra were recorded on a 300 MHz Bruker Avance DPX 300 NMR spectrometer,

a 400 MHz Bruker Avance Ultrashield Plus NMR spectrometer, or a 600 MHz Varian Unity Inova NMR spectrometer. Chemical shifts (δ) were reported in parts per million (ppm) referenced to an internal standard of residual proteo-solvent (^{1}H NMR, ^{13}C NMR): $CDCl_3$ (7.26, 77.16), CD_3OD (3.31, 49.00) or [D_6]DMSO (2.50, 39.52).[22] Multiplicity is quoted as app. (apparent), br. (broad), s (singlet), d (doublet), t (triplet), q (quartet), p (pentet) and m (multiplet). Coupling constants (*J*) are given in Hertz (Hz). Low resolution mass spectrometry (LRMS) analyses were performed using a Micromass Platform II single quadrupole mass spectrometer equipped with an atmospheric pressure (ESI/APCI) ion source. Sample management was facilitated by an Agilent 1100 series high performance liquid chromatography (HPLC) system using MassLynx version 3.5 software. High resolution mass spectrometry (HRMS) analyses were carried out on a Waters Micromass LCT Premier XE Orthogonal Acceleration time-of-flight (TOF) mass spectrometer coupled to an Alliance 2795 Separation Module using MassLynx version 4.1 software. Liquid chromatography–mass spectrometry (LCMS) was performed on an Agilent 1200 Series Separation Module fitted with a 6120 quadropole detector and a Phenomenex Luna C8(2) 100 Å (50×4.6 mm, internal diameter) 5 μm column. Samples were run in a gradient of 5–100% buffer B in buffer A (buffer A: 0.1% aq formic acid; buffer B: 80% CH_3CN, 19.9% water, 0.1% formic acid) over 4 min, followed by isocratic 100% buffer B for 3 min then a gradient of 100–0% buffer B over 3 min at a flow rate of 0.5 mL min^{-1}. Agilent Chemstation software (version B.04.01) managed the running and processing of samples. Analytical reversed phase (RP) HPLC was acquired on a Waters Millenium 2690 system fitted with a Phenomenex Luna C8 100 Å (50×4.6 mm, internal diameter) 5 μm column with UV detection at 254 nm. Samples were run in a gradient of 20–100% buffer B in buffer A (buffer A: 0.1% aq trifluoroacetic acid; buffer B: 80% CH_3CN, 19.9% water, 0.1% trifluoroacetic acid) over 10 min, followed by isocratic 100% buffer B for 1 min then a gradient of 100–20% buffer B over 1 min followed by isocratic 20% buffer B for 10 min at a flow rate of 1.0 mL/minute. EmPowerPro managed the running and processing of samples. Microwave chemistry was performed using a Biotage Initiator Microwave Reactor according to manufacturer's instructions.

4-(2-(4-Fluorophenyl)thiophen-3-yl)pyridine (2): To a solution of 2,3-dibromothiophene (2.38 mL, 20.7 mmol) in *N*,*N*-dimethylformamide (DMF) (160 mL) was added 4-fluorophenylboronic acid (2.89 g, 20.7 mmol), $Na_2CO_3{\cdot}H_2O$ (12.3 g, 99.2 mmol), and H_2O (40 mL). The reaction mixture was bubbled with nitrogen for 15 min. $PdCl_2(PPh_3)_2$ (0.725 g, 1.03 mmol) was added, and the reaction mixture was heated at 70 °C for 3 h. Pyridine-4-boronic acid (3.81 g, 31.0 mmol) and additional $PdCl_2(PPh_3)_2$ (0.725 g, 1.03 mmol) were added, and the reaction mixture was heated at 120 °C for 16 h. The reaction mixture was cooled to RT, passed through a plug of silica, and washed with EtOAc (160 mL). The organic layer was washed with H_2O (5×100 mL), then brine (50 mL), dried over $MgSO_4$, and filtered. The organic layer was evaporated in vacuo and purified by column chromatography using a gradient elution (0–50% EtOAc/petroleum spirits) to afford a pale yellow solid. Recrystallisation from Et_2O gave thiophene **2** ($C_{15}H_{10}FNS$: M_r=255.31) as a white powder (3.81 g, 71%): mp 95.8–97.6 °C; ^{1}H NMR (400 MHz, $CDCl_3$): δ=8.51 (br. app. d, J=5.6 Hz, 2H), 7.37 (d, J=5.2 Hz, 1H), 7.28–7.23 (m, 2H), 7.18 (d, J=5.3 Hz, 1H), 7.16–7.15 (m, 2H), 7.04–6.98 ppm (m, 2H); ^{13}C NMR (101 MHz, $CDCl_3$): δ=162.3 (d, $^1J_{CF}$=248.5 Hz), 149.8, 143.6, 139.7, 135.1, 130.9 (d, $^3J_{CF}$=8.1 Hz), 129.33 (d, $^4J_{CF}$=3.4 Hz), 129.27, 125.0, 123.4, 115.6 ppm (d, $^2J_{CF}$=21.7 Hz); HRMS-ToF-ESI: *m/z* [M+H]$^+$ calcd for $C_{15}H_{11}FNS^+$: 256.0591, found 256.0589; LCMS (ESI): t_R=4.9 min, 256.1 [M+H]$^+$; RP-HPLC: t_R=6.5 min, 99%.

4-(2-(4-Fluorophenyl)-4,5-diiodothiophen-3-yl)pyridine (3): To a solution of compound **2** (0.861 g, 3.37 mmol) in AcOH (18 mL) was added $Hg(OAc)_2$ (3.23 g, 10.1 mmol). The solution was heated at 70 °C for 16 h. Concurrently, I_2 (5.14 g, 20.2 mmol) and KI (3.36 g, 20.2 mmol) were dissolved in H_2O (38 mL) over 16 h in a separate round-bottom flask. After 16 h, the AcOH mixture was concentrated in vacuo and poured into ice water (100 mL). The resulting white precipitate was filtered and washed with H_2O then Et_2O to afford the mercuric acetate intermediate as a white powder. The intermediate was added to the KI_3 solution. THF (1 mL) was added to break the surface tension, and the mixture was stirred at 25 °C for 16 h. Saturated $Na_2S_2O_3$ (100 mL) was added, and the resulting yellow solid was filtered and washed with H_2O (50 mL). The solid was dissolved in THF/EtOAc (100 mL) and washed further with saturated $Na_2S_2O_3$ (3×50 mL). The organic extract was dried over $MgSO_4$, filtered, and concentrated in vacuo to afford thiophene **3**. Recrystallisation from THF/EtOH (1:1) afforded compound **3** ($C_{15}H_8FI_2NS$: M_r=507.10) as yellow crystals (1.39 g, 81%): mp 212.8 °C (decomp.); ^{1}H NMR (400 MHz, [D_6]DMSO): δ=8.59–8.58 (m, 2H), 7.20–7.12 ppm (m, 6H); ^{13}C NMR (101 MHz, [D_6]DMSO): δ=162.0 (d, $^1J_{CF}$=247.0 Hz), 149.7, 145.1, 145.0, 140.1, 130.9 (d, $^3J_{CF}$=8.5 Hz), 128.4 (d, $^4J_{CF}$=3.2 Hz), 125.5, 115.8 (d, $^2J_{CF}$=21.9 Hz), 101.8, 87.6 ppm; HRMS-ToF-ESI: *m/z* [M+H]$^+$ calcd for $C_{15}H_9FI_2NS^+$: 507.8524, found 507.8521; LCMS (ESI): t_R=6.4 min, 507.9 [M+H]$^+$; RP-HPLC: t_R=8.4 min, >99%.

(But-3-yn-1-yloxy)(*tert*-butyl)dimethylsilane (5):[23] Compound **5** was synthesised using a similar procedure by Nadeau et al.[23] To a solution of 3-butyn-1-ol (3.00 g, 42.8 mmol) in CH_2Cl_2 (60 mL) was added imidazole (7.28 g, 107 mmol) and cooled to 5 °C. TBSCl (6.45 g, 42.8 mmol) was added and the reaction mixture was stirred at 25 °C for 16 h. CH_2Cl_2 (100 mL) was added and the mixture was washed with H_2O (2×50 mL) and brine (50 mL). The organic layer was dried over $MgSO_4$, filtered, and concentrated in vacuo to afford compound **5** (7.73 g, 98%) as a colourless oil. **5**: $C_{10}H_{20}OSi$ (M_r=184.35); ^{1}H NMR (400 MHz, $CDCl_3$): δ=3.74 (t, J=7.1 Hz, 2H), 2.40 (td, J=7.1, 2.7 Hz, 2H), 1.95 (t, J=2.7 Hz, 1H), 0.90 (s, 9H), 0.07 (s, 6H); ^{13}C NMR (101 MHz, $CDCl_3$): δ=81.6, 69.4, 61.9, 26.0, 23.0, 18.4, −5.2 ppm.

4-(5-(4-((*tert*-Butyldimethylsilyl)oxy)but-1-yn-1-yl)-2-(4-fluorophenyl)-4-iodothiophen-3-yl)pyridine (6): ***Negishi coupling***: To a solution of alkyne **5** (2.06 mL, 9.97 mmol) in THF (15 mL) was added dropwise *n*BuLi (1.2 M, 8.3 mL, 10 mmol) at 0 °C. The reaction mixture was stirred for 15 min. $ZnCl_2$ (1.63 g, 12.0 mmol) was added, and the reaction mixture was stirred at 0 °C for 15 min, then allowed to warm to 25 °C for 15 min, at which time the zinc had dissolved. Concurrently, compound **3** (1.23 g, 2.43 mmol) was dissolved in THF (18 mL), and nitrogen was bubbled through the solution for 30 min. The metallated alkyne solution was added dropwise to the thiophene solution followed by addition of tetrakis(triphenylphosphine)palladium(0) (0.283 g, 0.245 mmol). The mixture was stirred at 25 °C for 70 h. Saturated NH_4Cl (7.5 mL) was added, and the mixture was stirred for 15 min. EtOAc (150 mL) was added and the mixture was washed with saturated Na_2CO_3 (3×40 mL) and brine (3×40 mL). The organic layer was dried over $MgSO_4$, filtered, and concentrated in vacuo. The product was purified by column chromatography using a gradient elution (0–50% EtOAc/petroleum spirits) to afford thiophene **6** as a pale yellow solid (1.27 g, 94%). ***Sonogashira coupling***: To a solution of compound **3** (1.30 g, 2.56 mmol) in THF (13 mL) was added alkyne **5** (800 μL, 3.88 mmol), PPh_3 (0.010 g, 0.038 mmol), CuI (0.027 g, 0.142 mmol), and bis(triphenylphosphine)palladium(II) dichloride

(0.093 g, 0.132 mmol). The reaction mixture was bubbled with nitrogen for 15 min and heated at 120 °C for 2 h. The reaction mixture was diluted with EtOAc (100 mL) and washed with H_2O (3× 50 mL) and brine (50 mL), dried over $MgSO_4$, filtered and concentrated in vacuo. The resulting oil was purified by column chromatography using a gradient elution (0–50% EtOAc/petroleum spirits) to afford compound **6** as a white solid. Trituration with petroleum spirits gave compound **6** ($C_{25}H_{27}FINOSSi$: $M_r = 563.54$) as a white powder (1.19 g, 82%): mp 96.6–97.7 °C; ^{1}H NMR (400 MHz, $CDCl_3$): $\delta = 8.60$ (br. app. d, $J = 4.8$ Hz, 2H), 7.13–7.11 (m, 2H), 7.10–7.05 (m, 2H), 6.94–6.89 (m, 2H), 3.87 (t, $J = 6.9$ Hz, 2H), 2.73 (t, $J = 6.9$ Hz, 2H), 0.92 (s, 9H), 0.11 ppm (s, 6H); ^{13}C NMR (101 MHz, $CDCl_3$): $\delta =$ 162.8 (d, $^1J_{CF} = 249.8$ Hz), 150.1, 144.9, 140.1, 138.3, 130.9 (d, $^3J_{CF} =$ 8.3 Hz), 128.6 (d, $^4J_{CF} = 3.4$ Hz), 125.7, 115.9 (d, $^2J_{CF} = 21.9$ Hz), 96.9, 91.8, 75.7, 61.6, 26.1, 24.5, 18.5, −5.1 ppm (n.b. Missing a quaternary carbon resonance in the ^{13}C NMR); HRMS-ToF-ESI: *m/z* $[M+H]^+$ calcd for $C_{25}H_{28}FINOSSi^+$: 564.0684, found 564.0701; LCMS (ESI): $t_R = 7.8$ min, 564.1 $[M+H]^+$; RP-HPLC: $t_R = 10.9$ min, 97%.

General procedure for Suzuki coupling: To a solution of thiophene **6** (100 mg, 1.0 equiv) in THF (3 mL) was added the boronic acid/pinacol ester (3.0 equiv) and Na_2CO_3 (1 M, 1 mL) in a 2–5 mL microwave vial. The reaction mixture was bubbled with nitrogen for 15 min. Bis(triphenylphosphine)palladium(II) dichloride (0.10 equiv) was added, the vial was capped, and the mixture was heated at 100 °C for 90 min in the microwave. The mixture was extracted with Et_2O (3×10 mL) and concentrated in vacuo. The product was purified by column chromatography.

General procedure for TBS deprotection: To the TBS-protected starting material (100 mg, 1.0 equiv) in MeOH (10 mL) was added NH_4F (3.0–4.0 equiv). The reaction mixture was heated at reflux for 16 h. The crude product was concentrated, diluted with EtOAc (20 mL), and washed with H_2O (3×10 mL). The organic fraction was dried over $MgSO_4$, filtered, and concentrated in vacuo. The crude product was purified by column chromatography.

Methyl 3-(2-(4-((*tert*-butyldimethylsilyl)oxy)but-1-yn-1-yl)-5-(4-fluorophenyl)-4-(pyridin-4-yl)thiophen-3-yl)benzoate (8): Compound **8** was synthesised using the general method for Suzuki coupling from thiophene **6** (250 mg, 0.444 mmol) and 3-(methoxycarbonyl)phenylboronic acid (240 mg, 1.33 mmol). Purification using gradient column chromatography (20–50% EtOAc/petroleum spirits) gave compound **8** ($C_{33}H_{34}FNO_3SSi$: $M_r = 571.78$) as a yellow solid (226 mg, 89%): ^{1}H NMR (400 MHz, $CDCl_3$): $\delta = 8.38$–8.36 (m, 2H), 7.96–7.95 (m, 1H), 7.94–7.91 (m, 1H), 7.29 (app. td, $J = 7.7$, 0.5 Hz, 1H), 7.23–7.21 (m, 1H), 7.15–7.10 (m, 2H), 6.98–6.92 (m, 2H), 6.83–6.82 (m, 2H), 3.87 (s, 3H), 3.70 (t, $J = 7.1$ Hz, 2H), 2.56 (t, $J = 7.1$ Hz, 2H), 0.87 (s, 9H), 0.04 ppm (s, 6H); LCMS (ESI): $t_R =$ 7.6 min, 572.3 $[M+H]^+$.

Methyl 3-(5-(4-fluorophenyl)-2-(4-hydroxybut-1-yn-1-yl)-4-(pyridin-4-yl)thiophen-3-yl)benzoate (29): Compound **29** was synthesised from compound **8** (462 mg, 0.808 mmol) following the general procedure for TBS deprotection. Purification by column chromatography in 10% MeOH/$CHCl_3$ afforded thiophene **29** ($C_{27}H_{20}FNO_3S$: $M_r = 457.52$) as a white powder (361 mg, 98%): mp 148.6–150.1 °C; ^{1}H NMR (400 MHz, [D$_6$]DMSO): $\delta = 8.39$–8.37 (m, 2H), 7.86–7.82 (m, 2H), 7.41 (app. t, $J = 7.7$ Hz, 1H), 7.32 (app. dt, $J = 7.7$, 1.6 Hz, 1H), 7.26–7.21 (m, 2H), 7.19–7.14 (m, 2H), 6.97–6.96 (m, 2H), 4.87 (t, $J = 5.6$ Hz, 1H), 3.81 (s, 3H), 3.47 (td, $J = 6.9$, 5.7 Hz, 2H), 2.52–2.48 ppm (m, 2H); ^{13}C NMR (101 MHz, [D$_6$]DMSO): $\delta =$ 165.8, 162.0 (d, $^1J_{CF} = 247.0$ Hz), 149.6, 143.8, 142.9, 139.0, 135.1, 134.6, 134.3, 131.3 (d, $^3J_{CF} = 8.5$ Hz), 130.5, 129.4, 128.6, 128.6 (d, $^4J_{CF} = 5.4$ Hz), 128.3, 125.5, 119.9, 115.9 (d, $^2J_{CF} = 21.9$ Hz), 96.2, 73.3, 59.4, 52.2, 23.6 ppm; HRMS-ToF-ESI: *m/z* $[M+H]^+$ calcd for $C_{27}H_{21}FNO_3S^+$: 458.1221, found 458.1236; LCMS (ESI): $t_R = 5.4$ min, 458.2 $[M+H]^+$; RP-HPLC: $t_R = 7.3$ min, >99%.

Biological assays

Fluorescence polarisation (FP) assay: FP signals were measured with a PHERAstar microplate reader (BMG Labtech) using black, low-binding half-area 96-well plates (Corning). Each binding data point was carried out in duplicate or triplicate. Data were recorded in millipolarisation (mP) units and measured at an excitation wavelength of 485 nm and an emission wavelength of 520 nm. Tris assay buffer was used in all binding experiments and consisted of 10 mM Tris, 50 nM KCl, and 3.5 mM CHAPS at pH 8.0. The recombinant inactive and active His-tag p38α MAPK used in the ligand binding assays were prepared as described by Bukhtiyarova et al.[24]

Determination of the K_d value for the fluorescently labelled ligand: The method used to determine the K_d value for the fluoroprobe was similar to the method by Munoz et al.[16] 5 nM of the fluoroprobe was incubated at RT for 1 h with increasing concentrations of inactive p38α MAPK (0–1000 nM) in the presence of 10% DMSO. The K_d value was calculated from three independent experiments with GraphPad Prism using nonlinear regression analysis. To determine the affinity of the fluoroprobe to active p38α MAPK, 5 nM of fluoroprobe was incubated at RT for 2 h with increasing concentrations of active p38α MAPK (0–500 nM) in the presence of 10% DMSO.

Ligand binding experiments: Test compounds were prepared from DMSO stocks (10 mM). To determine the K_i values, the test compounds (final concentration ranging from 500 μM–10 nM), 5 nM of fluoroprobe and 50 nM of inactive p38α MAPK were added to each well. Plates were incubated at RT for 1 h and FP signals were recorded. For binding experiments to active p38α MAPK, the FP signals were recorded after 2 h incubation at RT. Data (IC_{50}) were calculated with GraphPad Prism using nonlinear regression analysis and are presented as mean ± standard error (SEM) from two to three independent experiments performed in duplicates.

Neonatal cardiac fibroblast (NCF) culture: The investigation conformed to the Guide for the Care and Use of Laboratory Animals published by the US National Institutes of Health (PHS Approved Animal Welfare Assurance #A5587–01). All animal usage was also approved by the Alfred Medical Research and Education Precinct (AMREP) Animal Ethics Committee (AEC) in accordance with National Health and Medical Research Council (NHMRC) guide for the care and use of laboratory animals (AEC # E/0981/2010M). Sprague–Dawley rat neonatal cardiac fibroblasts (NCFs) were isolated from one- to two-day-old pups with enzymatic digestion as described in detail previously.[18,25] NCFs were seeded and maintained in high-glucose (25 mM) Dulbecco's modified Eagle medium (DMEM) (Invitrogen, Mount Waverley, Australia) in the presence of 1% antibiotic/antimycotic (Invitrogen, Mount Waverley, Australia) and 10% foetal bovine serum (JRH biosciences, Lenexa, USA). NCFs were used at passage two.[18,26]

NCF collagen synthesis assay: NCF collagen synthesis was determined by ^{3}H-proline incorporation as described previously.[18,26] NCFs were seeded at a density of 50,000 cells/well in 12-well plates and incubated (37 °C, 5% CO_2) overnight before serum starvation with 0.5% bovine serum albumin (BSA) for 48 h. Cells were then pre-treated in the presence or absence of test compounds (0.1, 1,

3, or 10 μM) for 2 h before stimulation with 100 nM AngII in the presence of 0.5% BSA and addition of 1 μCi of ^{3}H-proline to each well. After 48 h of further incubation, cells were harvested by 10% trichloroacetic acid (TCA) preparation, and ^{3}H-proline incorporation was determined as previously described.[26–27]

Acknowledgements

This work was supported by scholarships and grants from the Australian National Health and Medical Research Council (Development grant: 519585), the Sydney Medical School–The University of Sydney (Australia) (Early Career Research Scheme grant to L.M.), and the Australian Government through an Australian Postgraduate Award (APA) scholarship (to N. B. V.).

Keywords: cardiac remodelling · fibrosis · molecular docking · p38α mitogen-activated protein kinase (MAPK) · structure–activity relationships (SAR)

[1] a) G. L. Schieven, *Curr. Top. Med. Chem.* **2005**, *5*, 921 – 928; b) S. Kumar, J. Boehm, J. C. Lee, *Nat. Rev. Drug Discov.* **2003**, *2*, 717 – 726; c) Y. Keshet, R. Seger, *Methods Mol. Biol.* **2010**, *661*, 3 – 38.

[2] a) H. Y. Yong, M. S. Koh, A. Moon, *Expert Opin. Invest. Drugs* **2009**, *18*, 1893 – 1905; b) A. Cuenda, S. Rousseau, *Biochim. Biophys. Acta* **2007**, *1773*, 1358 – 1375.

[3] a) T. M. Behr, C. P. Doe, J. Haisong, R. N. Willette in *Inflammation and Cardiac Diseases* (Eds.: G. Z. Feuerstein, P. Libby, D. L. Mann), Birkhäuser, Basel, **2003**, pp. 293 – 312; b) M. S. Marber, B. Rose, Y. Wang, *J. Mol. Cell. Cardiol.* **2011**, *51*, 485 – 490.

[4] a) F. See, W. Thomas, K. Way, A. Tzanidis, A. Kompa, D. Lewis, S. Itescu, H. Krum, *J. Am. Coll. Cardiol.* **2004**, *44*, 1679 – 1689; b) Z. Li, T. T. Tran, J. Y. Ma, G. O'Young, A. M. Kapoun, S. Chakravarty, S. Dugar, G. Schreiner, A. A. Protter, *J. Cardiovasc. Pharmacol.* **2004**, *44*, 486 – 492; c) Y. H. Liu, D. Wang, N. E. Rhaleb, X. P. Yang, J. Xu, S. S. Sankey, A. E. Rudolph, O. A. Carretero, *J. Card. Failure* **2005**, *11*, 74 – 81; d) A. R. Kompa, F. See, D. A. Lewis, A. Adrahtas, D. M. Cantwell, B. H. Wang, H. Krum, *J. Pharmacol. Exp. Ther.* **2008**, *325*, 741 – 750.

[5] a) K. P. Wilson, M. J. Fitzgibbon, P. R. Caron, J. P. Griffith, W. Chen, P. G. McCaffrey, S. P. Chambers, M. S. Su, *J. Biol. Chem.* **1996**, *271*, 27696 – 27700; b) Z. Wang, P. C. Harkins, R. J. Ulevitch, J. Han, M. H. Cobb, E. J. Goldsmith, *Proc. Natl. Acad. Sci. USA* **1997**, *94*, 2327 – 2332.

[6] P. Traxler, *Expert Opin. Ther. Pat.* **1998**, *8*, 1599 – 1625.

[7] a) Z. Wang, B. J. Canagarajah, J. C. Boehm, S. Kassisa, M. H. Cobb, P. R. Young, S. Abdel-Meguid, J. L. Adams, E. J. Goldsmith, *Structure* **1998**, *6*, 1117 – 1128; b) J. Lisnock, A. Tebben, B. Frantz, E. A. O'Neill, G. Croft, S. J. O'Keefe, B. Li, C. Hacker, S. de Laszlo, A. Smith, B. Libby, N. Liverton, J. Hermes, P. LoGrasso, *Biochemistry* **1998**, *37*, 16573 – 16581.

[8] T. F. Gallagher, G. L. Seibel, S. Kassis, J. T. Laydon, M. J. Blumenthal, J. C. Lee, D. Lee, J. C. Boehm, S. M. Fier-Thompson, J. W. Abt, M. E. Soreson, J. M. Smietana, R. F. Hall, R. S. Garigipati, P. E. Bender, K. F. Erhard, A. J. Krog, G. A. Hofmann, P. L. Sheldrake, P. C. McDonnell, S. Kumar, P. R. Young, J. L. Adams, *Bioorg. Med. Chem.* **1997**, *5*, 49 – 64.

[9] a) S. P. Davies, H. Reddy, M. Caivano, P. Cohen, *Biochem. J.* **2000**, *351*, 95 – 105; b) K. Godl, J. Wissing, A. Kurtenbach, P. Habenberger, S. Blencke, H. Gutbrod, K. Salassidis, M. Stein-Gerlach, A. Missio, M. Cotten, H. Daub, *Proc. Natl. Acad. Sci. USA* **2003**, *100*, 15434 – 15439; c) J. L. Norris, K. P. Williams, W. P. Janzen, C. N. Hodge, L. J. Blackwell, I. G. Popa-Burke, *Lett. Drug Des. Discov.* **2005**, *2*, 516 – 521.

[10] R. L. Thurmond, S. A. Wadsworth, P. H. Schafer, R. A. Zivin, J. J. Siekierka, *Eur. J. Biochem.* **2001**, *268*, 5747 – 5754.

[11] S. A. Wadsworth, D. E. Cavender, S. A. Beers, P. Lalan, P. H. Schafer, E. A. Malloy, W. Wu, B. Fahmy, G. C. Olini, J. E. Davis, J. L. Pellegrino-Gensey, M. P. Wachter, J. J. Siekierka, *J. Pharmacol. Exp. Ther.* **1999**, *291*, 680 – 687.

[12] D. M. Goldstein, A. Kuglstatter, Y. Lou, M. J. Soth, *J. Med. Chem.* **2010**, *53*, 2345 – 2353.

[13] M. Fujita, T. Hirayama, N. Ikeda, *Bioorg. Med. Chem.* **2002**, *10*, 3113 – 3122.

[14] S. A. Beers, E. Malloy, M. P. Wachter, W. Wu, *Substituted Imidazoles Useful in the Treatment of Inflammatory Diseases*, WO 98/47892, Oct. 29, **1998**.

[15] N. B. Vinh, J. S. Simpson, P. J. Scammells, D. K. Chalmers, *J. Comput.-Aided Mol. Des.* **2012**, *26*, 409 – 423.

[16] L. Munoz, R. Selig, Y. T. Yeung, C. Peifer, D. Hauser, S. Laufer, *Anal. Biochem.* **2010**, *401*, 125 – 133.

[17] Y. Y. Zhang, J. W. Wu, Z. X. Wang, *J. Biol. Chem.* **2011**, *286*, 16150 – 16162.

[18] S. Lekawanvijit, A. Adrahtas, D. J. Kelly, A. R. Kompa, B. H. Wang, H. Krum, *Eur. Heart J.* **2010**, *31*, 1771 – 1779.

[19] M. van Eickels, C. Grohe, K. Lobbert, M. Stimpel, H. Vetter, *Naunyn-Schmiedeberg's Arch. Pharmacol.* **1999**, *359*, 394 – 399.

[20] M. Vogtherr, K. Saxena, S. Hoelder, S. Grimme, M. Betz, U. Schieborr, B. Pescatore, M. Robin, L. Delarbre, T. Langer, K. U. Wendt, H. Schwalbe, *Angew. Chem. Int. Ed.* **2006**, *45*, 993 – 997; *Angew. Chem.* **2006**, *118*, 1008 – 1012.

[21] H. M. Berman, J. Westbrook, Z. Feng, G. Gilliland, T. N. Bhat, H. Weissig, I. N. Shindyalov, P. E. Bourne, *Nucleic Acids Res.* **2000**, *28*, 235 – 242.

[22] H. E. Gottlieb, V. Kotlyar, A. Nudelman, *J. Org. Chem.* **1997**, *62*, 7512 – 7515.

[23] C. Nadeau, V. G. Gund, C. Spino, *Novel Resins Bearing a Chiral Auxiliary for the Construction of Small Chiral Organic Molecules*, CA 2413713, June 6, **2004**.

[24] M. Bukhtiyarova, K. Northrop, X. Chai, D. Casper, M. Karpusas, E. Springman, *Protein Expression Purif.* **2004**, *37*, 154 – 161.

[25] a) P. Simpson, *Circ. Res.* **1985**, *56*, 884 – 894; b) E. A. Woodcock, B. H. Wang, J. F. Arthur, A. Lennard, S. J. Matkovich, X. J. Du, J. H. Brown, R. D. Hannan, *J. Biol. Chem.* **2002**, *277*, 22734 – 22742.

[26] B. H. Wang, M. C. Bertucci, J. Y. Ma, A. Adrahtas, R. Y. Cheung, H. Krum, *Clin. Exp. Pharmacol. Physiol.* **2010**, *37*, 912 – 918.

[27] A. R. Kompa, B. H. Wang, G. Xu, Y. Zhang, P. Y. Ho, S. Eisennagel, R. K. Thalji, J. P. Marino, Jr., D. J. Kelly, D. J. Behm, H. Krum, *Int. J. Cardiol.* **2013**, *167*, 210 – 219.

Received: September 29, 2014
Published online on November 11, 2014